Electronic Supplementary Material (ESI) for Green Chemistry.

Support Information

Chemicals:

Potassium borohydride (KBH_4), sodium oxalate (NaC_2O_4) and silver nitrate ($AgNO_3$) were all analytically pure. The multiwall carbon nanotubes (MWCNTs) were obtained from Timesnano, and chloroplatinic acid hydrate (H_2PtCl_6, 37%-40% Pt) was bought from Alfa Aesar.

Experimental details:

Preparation of the Ag@C nanocables.

In a typical synthesis, 1.1 mL of glycerol and 0.2548g of $AgNO_3$ were added into 35 mL of H_2SO_4 aqueous solution under a vigorous stirring for 2 hours, and then it was transferred into a 50 mL Teflon-lined stainless-steel autoclave. The autoclave was sealed, heated at 180℃ for 10 hours, and then air-cooled to room temperature. After reaction, the product was collected by filtration and washed several times with double-distilled water (DD water). The product was dried at 40^{o}C under vacuum for 8 hours to obtain a powder. Then, the collected powder was heated up to 600 °C for 3 hours in a tube furnace in nitrogen atmosphere. Finally, the powder was boiled in 2 M KOH solution for 2 hours, washed copiously with DD water and dried at 40 °C under vacuum condition for 8 hours to obtain the final product, which is denoted as Ag@C nanocables in this paper.

Synthesis of Pt/Ag@C nanocables catalyst

To deposit Pt nanoparticles on Ag@C nanocable support, 100 mg of sodium oxalate and 40 mg of pre-treated Ag@C nanocable powder were added into 100 mL ethanol-water (1:1, v/v) solution, and ultrasonically treated for 30 minutes. Subsequently, H_2PtCl_6 (10 mg Pt in 5 mL DD water) aqueous solution was added into the system and stored at room temperature overnight. A freshly prepared KBH_4 solution (100 mg in 100 mL DD water) was added dropwise into the above solution under moderate stirring for 4 hours to make sure the completely reduction of H_2PtCl_6. The whole process was operated at room temperature. Finally, the product was collected by filtration and washed several times, then dried at 40 ^{o}C under vacuum for 12 hours to obtain the final catalyst product. This catalyst material is donated to Pt/Ag@C in this paper.

Comparison experiments

For a comparison, commercial MWCNTs and C-shell were also used as the supports for Pt particles, and their corresponding catalysts were also prepared using similar procedures as those for Pt/Ag@C catalyst. And the corresponding catalyst is donated to Pt/MWCNTs and Pt/C-shell in this paper.

Structure and morphology characterization:

Morphologies and strictures of the catalyst samples were characterized by TEM (JEOL-100CX) at 200 kV. The crystal structures of the catalyst samples were analysed by XRD recorded on a D/max-2200/PC X-ray diffractometer with Cu Kα radiation source. For composition analysis, both FESEM images and EDS results were obtained with ZEISS SUPRA 40 and X-MAX 20.

Electrochemical Investigation:

The electrochemical measurements in this study were conducted using a conventional three-electrode electrochemical cell by a CHI 660E electrochemical workstation. A glassy carbon electrode (3 mm o.d.) coating with different catalysts as described above was used as the working electrode, a saturated calomel electrode (SCE) was employed as the reference electrode and a Pt foil (1 cm^2) as the counter electrode. The working electrode was cleaned with DD water, and dried at room temperature for the preparation of the catalyst layer on it. Generally, 3 mg of catalyst sample was ultrasonically dispersed into 0.3 mL of ethanol and 30 μL of 5 wt% perfluorosulfonic acid (PFSA) solution to obtain homogeneous ink followed by dropping 5 μL of ink onto a freshly polished glassy carbon electrode (3mm o.d.).The metal loading is 0.86 $mg\cdot cm^{-2}$. The cyclic voltammetric (CV) and chronoamperometric curves for glycerol electrooxidation experiments were carried out in N_2-saturated 1 M KOH containing 1M glycerol. All electrochemical experiments were performed at 25±1℃.

Computational details

All Spin-polarized calculations presented in this work were performed employing the periodic density functional theory (DFT) method implemented in the Vienna Ab-Initio Simulation Package (VASP). The ionic cores were represented by the projector augmented wave (PAW) potentials. The 2s2p, 2s2p, 4d5s, 5d6s electrons of carbon, oxygen, silver, platinum atoms were treated as the valence electrons. The exchange and correlation interactions among electrons were described at a level of the generalized gradient approximation (GGA), using the Perdew–Burke–Ernzerhof (PBE) functional. The Gaussian smearing method with a half-width of 0.05 eV was employed to accelerate convergence of electronic charge densities. The wave functions were expanded in plane waves with a cut off energy of 400 eV and the convergence criterion for the electronic self-consistent iteration was set to 10^{-5} eV. In this work we also applied a Van-der-Waals correction to investigate the interaction between the reactants or the intermediates and the Graphite support.

The stable graphite structure was consisted of stacked carbon-atom planes in which each atom was bonded to three other atoms to form a hexagonal network. In order to compute the equilibrium properties of bulk graphite, we employed the Monkhorst–Pack scheme and a 6×6×1 Γ-centered grid for the k-points sampling. After structure optimization of an initial atomic geometry with arbitrary lattice parameters via both the conjugate gradient algorithm and the quasi-Newton scheme, the equilibrium lattice constants were found to be a0=2.467 Å and c0=6.80 Å. The theoretical equilibrium in-plane lattice constant a0 was in an excellent agreement with the experimental value of 2.456 Å, suggesting that the DFT-GGA scheme could describe the strong covalent bonds in the hexagonal network structure fairly well. The interlayer lattice constant c0 also agreed reasonably well with the experimental value of 6.696 Å, especially considering that the adjacent layers in graphite were relatively far apart with only weak bonding between them. The graphite (0001) substrate was consisted of four carbon layers with (2×2) surface cells that contained eight carbon atoms per layer. The graphite(0001)/Ag sample was modeled with a (2x2) graphite (0001) film supported on the a (2x2) Ag (111) film, with the (111) planes of the Ag part parallel to the (0001) planes of graphite. The system was composed of four carbon layers and four silver (111) layers. The XRD experiments of graphite(0001)/Ag samples indicated that the Ag was composed mainly by (111) surface and the bond length of Ag-Ag is 2.89 Å. So we set the lattice parameter of graphite/Ag as 5.78 Å according to the Ag-Ag distance (2.89 Å). The lattice mismatch was 14.5%, with the C-C bond length of graphite (0001) on Ag (111) enlarged by 17.6 % compared with that of the graphite (0001) from 1.42 to 1.67 Å.

In the calculations, the atoms in two Ag layers in graphite/Ag were all allowed to relax. The atoms in the other layers, as well as the adsorbates were free to relax until the self-consistent force dropped to below 0.02 eV $Å^{-1}$. With the purpose of avoiding the interactions due to the artificial periodicity, a vacuum layer of at least 15 Å was used to separate the periodic images in the direction perpendicular to the surface. The Brillouin zone integration was performed using the Monkhorst–Pack scheme and a Γ-centered 6 × 6 × 1 grid for the k-points sampling. We also made a test with a 6 × 6 × 1 MP grid for comparison and found only tiny changes in energy (0.01 eV). A vacuum layer of 15 Å was used to separate the periodic images in the direction perpendicular to the surface. The Bader charge analysis scheme was applied to determine the atomic charges and charge transfer. The adsorption energy of a Pt atom on graphite or graphite/Ag was defined by

$$E_{ad} = E_{G\ (or\ G/Ag)} + E_{Pt} - E_{Pt/G\ (or\ Pt/G/Ag)}, \quad (1)$$

where $E_{Pt/G}$ and E_G are the total energies for the optimized equilibrium configurations of graphite (0001) or graphite(0001)/Ag with and without Pt adatom(X), respectively, and E_{Pt} is the total energy of the corresponding isolated Pt adatom in its ground state. The adsorption energy of CO on the Pt/G or Pt/G/Ag was defined by

$$E_{ad} = E_{Pt/G\ (or\ Pt/G/Ag)} + E_{CO} - E_{CO/Pt/G\ (or\ CO/\ Pt/G/Ag)}, \quad (2)$$

where $E_{CO/Pt/G\ (or\ CO/\ Pt/G/Ag)}$ and $E_{Pt/G\ (or\ Pt/G/Ag)}$ are the total energies of the optimized Pt/G or Pt/G/Ag with and without the CO adsorbate, respectively, and E_{CO} is the total energy of the corresponding isolated CO molecule in its ground state.

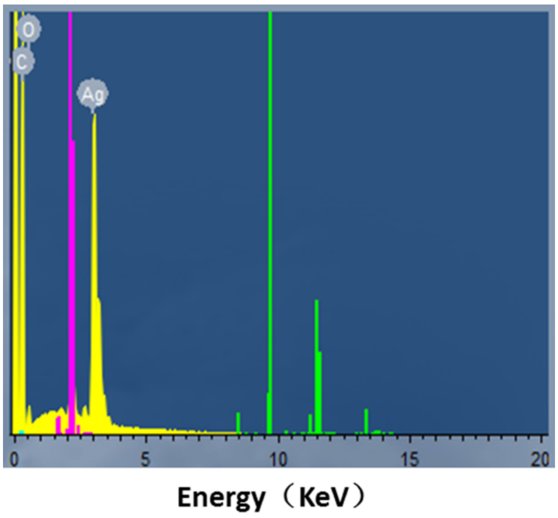

Fig. s1 EDS patterns of the Ag@C nanocables

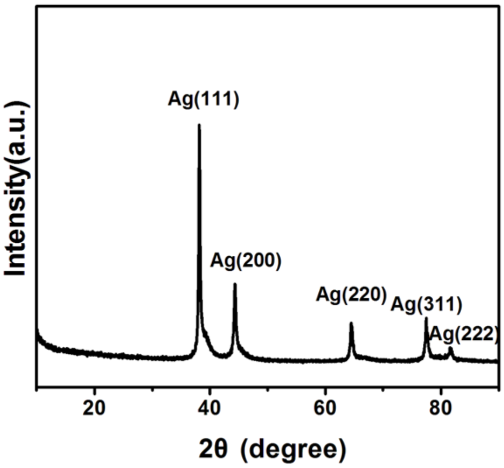

Fig. s2 XRD patterns of the Ag@C nanocables

In order to investigate the surface chemical states and elemental compositions, the Ag@C support was analyzed by X-ray photoelectron spectroscopy (XPS) and selected area electron diffraction (SAED) measurements. Fig. s3 shows the survey-scan spectra for the C 1s XPS signal of Ag@C, where three bands for this element (marked as C_I, C_{II} and C_{III} respectively) are analyzed. The dominant contributions are the C_I signal at 284.6 ± 0.1 eV for the C sp^2 bonds in the graphitic domains, and the C_{II} signal at 286.0 ± 0.2 eV could be assigned to the C-O single bonds which exist on the Ag@C surface. Finally, the C_{III} peak at 288.9 ± 0.1 eV can be considered as the contribution from the O–C–O bonds of carbonyl, which resides on the functional Ag@C substrate. It is found that 64.36 % C is from graphite structure, 29.75 % from C-O bonds and 5.89 % from O–C–O bonds. Fig. s4 shows the SAED pattern of Ag@C. As shown in Fig. s4, the SAED pattern has a typical diffraction ring profile, which indicates the crystalline structure of graphite, supporting the conclusion obtained from XPS studies.

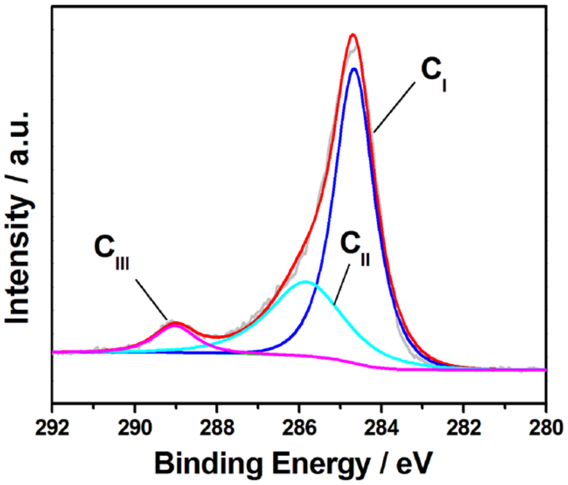

Fig. s3 Survey-scan spectra for the C 1s XPS signal of Ag@C.

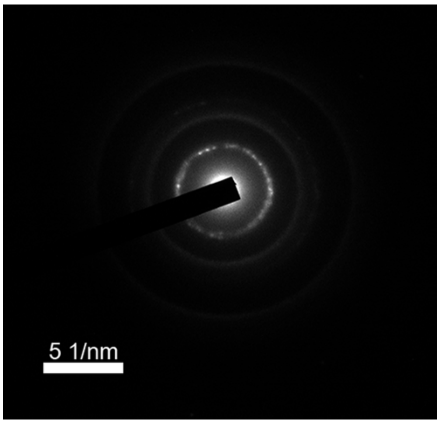

Fig. s4 SAED pattern of Ag@C

Fig. s5 shows the cyclic voltammograms obtained with CO adsorbed onto the catalysts (solid curves) and without CO adsorbed (dashed curves), of the as-prepared Pt/Ag@C and Pt/C-shell, respectively. It was performed in 0.5 M H_2SO_4 electrolyte at a scan rate of 50 mV·s^{-1}. The corresponding ECSA of the catalyst was obtained from Eq. (1) :

$$\mathrm{ECSA} = \frac{Q}{G \times 210} \quad (1)$$

Where Q is the charge of CO desorption-electrooxidation in microcoulomb (μC), G represents the total amount of Pt (μg) on the electrode, and 210 is the charge required to oxidize a monolayer of CO on the catalyst in μC·cm^{-2}. The ECAS value of the Pt/Ag@C catalyst (48.7 m^2 g^{-1}) is much larger than that of the Pt/C-shell catalyst (35.1 m^2 g^{-1}), leading to the higher electrocatalytic activity. The larger ECSA of the Pt/Ag@C catalyst might be attributed to the smaller size and better dispersion of the Pt nanoparticles.

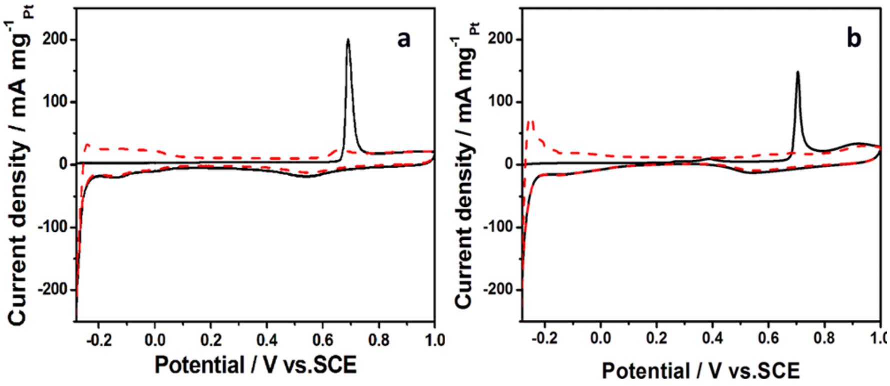

Fig. s5 Cyclic voltammograms for the oxidation of preadsorbed CO of the as-prepared catalysts from (a) Pt/Ag@C and (b) Pt/C-shell on glassy carbon electrode in 0.5M H_2SO_4 aqueous solution with a scan rate of 50 mV s^{-1} at 25 °C. Dashed curves were CVs for these electrodes without CO_{ad}.

TEM images of the Pt/Ag@C and Pt/C-shell were measured again after durability tests. The TEM images and the corresponding particle size distribution of the samples were shown in Fig. s6. From Fig. s6a, the obtained Pt nanoparticles with a little larger diameter (ca. 5.7 nm) are well-dispersed on the surface of the supports. From Fig. s6c, it can be seen that the obtained Pt nanoparticles on C-shell exhibit much larger diameters (ca. 6.9 nm) and serious agglomeration. The results demonstrate that this

Pt/Ag@C catalyst has not only a better catalytic activity but also a higher stability than that of Pt/C-shell under the same conditions.

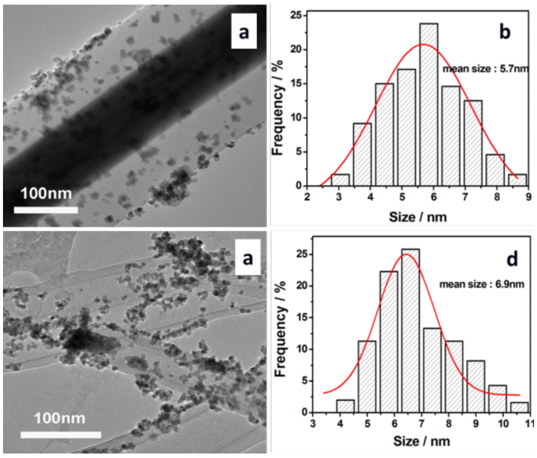

Fig.s6. TEM images and the corresponding size frequency curves of the resulting (a-b) Pt/Ag@C and (c-d) Pt/C-shell samples after durability tests.

In order to investigate the distribution and content of the catalysts, elemental mapping measurement were performed. Fig. s7 shows the FESEM images and the corresponding elemental mapping of the as-prepared catalysts from Pt/Ag@C (a) and Pt/C-shell (b). From the FESEM images, it can be seen that the Ag@C nanocables can be observed in Pt/Ag@C, while Ag nanowires disappear in Pt/C-shell. On the mapping images of the samples, a homogeneous distribution of C element can be clearly observed, and most Pt element is uniformly distributed on the surface of support. Obviously, a homogeneous distribution of Ag nanowire can be observed in Pt/Ag@C, while Ag nanowires disappear in Pt/C-shell. The result is in agreement with the TEM images.

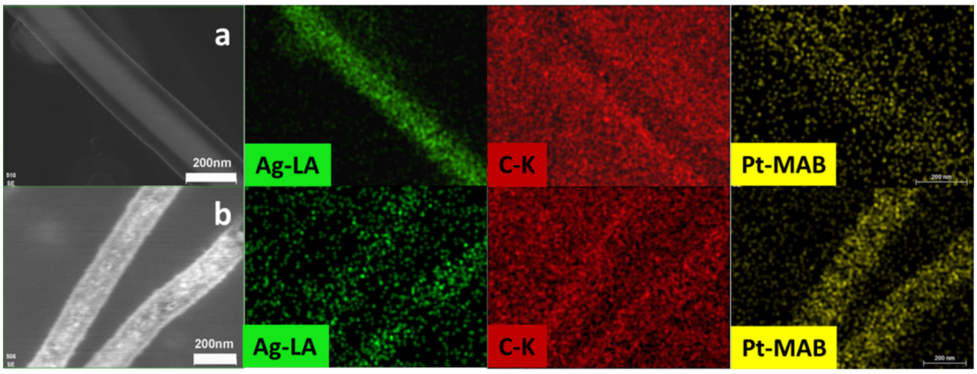

Fig. s7 FESEM images and corresponding chemical mapping of the as-prepared catalysts from Pt/Ag@C (a) and Pt/C-shell (b).